Available online at www.sciencedirect.com
ScienceDirect
Journal of Sound and Vibration 302 (2007) 962–980
JOURNAL OF SOUND AND VIBRATION
www.elsevier.com/locate/jsvi

Dynamic analysis of thin-walled closed-section beams

A. Prokić*, D. Lukić

Faculty of Civil Engineering Subotica, University of Novi Sad, Kozaracka 2a, 24000 Subotica, Serbia

Received 21 January 2006; received in revised form 9 January 2007; accepted 11 January 2007
Available online 26 February 2007

Abstract

The present paper considers the problem of dynamic behavior of thin-walled beams of arbitrary, closed cross-section, by means of an exact solution. Starting from Benscoter's theory, the differential equations of motion are derived by postulating the principle of the virtual work due to a variation of displacements. In the case of simply supported thin-walled beam, a closed-form solution for the coupled natural frequencies of free harmonic vibrations was derived. The method is illustrated by examples and results are compared with analytical results analyzed by Vlasov's theory as well as with FEM results.

1. Introduction

Thin-walled beams with closed cross-sections have been widely used in many engineering applications. These structures are characterized by a high stiffness to weight ratio and are applied when high torsional and bending rigidities are required. The vibration characteristics of those elements are of fundamental importance in the design of thin-walled structures. In the general case of arbitrary cross-section, lateral vibrations in two perpendicular directions are coupled with torsional and warping vibrations, and the frequency equations of such elements should be considered simultaneously.

In general, many research works are focused on the dynamic analysis of thin-walled closed beams with various degrees of rigor. Several methods are available in the range of finite element [1–5] and finite strip [6–9] to complex three-dimensional shell element model [10,11]. Some explicit analytical expressions for the frequency equations and mode shapes of a thin-walled beam with closed cross-section are also available in the literature. For example, Stavridis and Michaltsos [12] introduce non-dimensionalized eigenfrequency parameters, which govern the dynamic behavior of the thin-walled beam, but practical performance of the proposed solution, based on Vlasov's theory, requires the use of a numerical procedure supported by a computer program specially written for that purpose. An analytical method for free vibrations of box girders is presented by Kristek [13] but only for cross-sections with two planes of symmetry where flexural vibrations are separated from torsional vibration. Some researchers use the dynamic stiffness matrix method [14–16] to

*Corresponding author. Fax: +381 24 554 580.
E-mail address: aprokic@eunet.yu (A. Prokić).

0022-460X/$ - see front matter © 2007 Elsevier Ltd. All rights reserved.
doi:10.1016/j.jsv.2007.01.007

Nomenclature

a, b, c, d, e coefficients in the frequency equation
C origin of coordinate system
E modulus of elasticity
F area of cross-section
G shear modulus
h_{nP} distance from normal at arbitrary point on contour to pole
h_P distance from tangent at arbitrary point on contour to pole
$I_{xx}, I_{yy}, I_{\omega\omega}, I_{hh}, I_P$ geometrical properties of cross-section
$I^o_{\omega\omega}$ see Eq. (31)
K Saint Venant torsion constant
L length of element
m_x, m_y, m_P, m_ω external bending moments, torsional moment and bimoment per unit length
M_x, M_y bending moments
M_ω bimoment
n,s curvilinear coordinates
N axial force
O_1 starting point = point from which s is measured
p frequency
p_* see Eq. (39)
p_x, p_y, p_z externally applied loads per unit length in x, y and z directions, respectively
P shear center
t time
T_P total torsional moment
T_S Saint Venant torsional moment
u, v displacements of shear center in direction of x and y axes
u_*, v_*, w_* displacements of an arbitrary point on the contour
$\bar{U}$ work of actual stresses
U, V, Φ amplitudes of the transverse displacements and torsional rotation
V_x, V_y shear forces
w axial displacement of cross-section as rigid
$\bar{W}$ work of external load and inertia forces
x, y, z Cartesian coordinates
x_P, y_P coordinate of the shear centre
α angle between normal to the profile middle line and x-axis
γ_{zs}, γ_T shear strain
δ symbol of variation
$\boldsymbol{\varepsilon}$ strain tensor
ε_z longitudinal strain
ϑ warping parameter
λ_n $n\pi/L$
ξ_*, η_*, w_* displacements in normal, tangential and z directions
ρ specific mass
$\boldsymbol{\sigma}$ stress vector
σ_z normal stress
τ_{zs} shear stress
τ_T shear stress due to torsion
τ_V shear stress due to bending
$\tilde{\tau}$ Saint Venant shear flow for $G\varphi' = 1$
φ rotation of the cross-section around its shear centre
χ see Eq. (39)
ω warping function with pole at shear center
$()'$ $\partial()/\partial z$

solve free or forced vibration problems of thin-walled structures. The method is referred as an exact method since it is based on exact shape functions obtained from the exact solution of differential equations. As Moon-Young et al. [16] pointed out, this analytical method, however, is sometimes inefficient because analytical operations in solving a system of simultaneous ordinary differential equations with many variables may be too complex.

The objective of this work is to develop an exact analytical solution that enables the prediction of natural frequencies and mode shape of the free harmonic coupled vibrations of thin-walled beams with closed cross-sections accurately and efficiently. The expressions are concise and very simple and as such connvenient to be used by practicing engineer who does not need to go into detail of thin-walled beam theory. The Vlasov assumption for open profiles, setting the shear strain in the middle surface equal to zero, is not made because under this assumtion warping is excluded. Here, the warping function is described by a function given beforehand, and is the same as in the case of the Saint Venant's function of free-warping for beam with closed profiles. The function that defines the warping intensity represents a new unknown that may be derived as a function of the angle of rotation of the profile.

2. Basic theory

A straight thin-walled beam with a closed, generally multicellular cross-section is considered. In order to determine the geometry of the beam two coordinate systems are used. The first of these is an orthogonal Cartesian coordinate system for which the z-axis coincides with the longitudinal centroidal axis, while x and y coincide with principal axes of the section. The second coordinate system is a curvilinear coordinate system (n, s, z) where n is the normal coordinate measured along the normal to contour (middle line of a cross-section), and s is profile coordinate measured along the contour line from arbitrarily taken starting point O_1. The wall thickness is denoted by $t(s)$.

2.1. Suppositions

The theory of thin-walled beams with closed sections rests on the following simplifying assumptions:

1. The cross-section is perfectly rigid in its own plane (it is supposed that the cross-sections are stiffened by installing intermediate diaphragms in order to suppress all undesirable modes of distortion of the cross-sections).
2. The part of the shear strains in the middle surface of the wall, due to the bending moment, is negligible.
3. The distribution of warping deformation is the same as in the case of Saint Venant torsion.

In the technical theory of thin-walled beams with closed sections we assumed that normal stresses are constant over the entire thickness of the wall.

2.2. Kinematics and strains

According to the first assumption the cross-sectional behavior can be described by displacement components u and v of the shear center P as the pole and the rotation angle φ about the same pole, Fig. 1. From geometric considerations, normal and tangential displacements of an arbitrary point S_* with

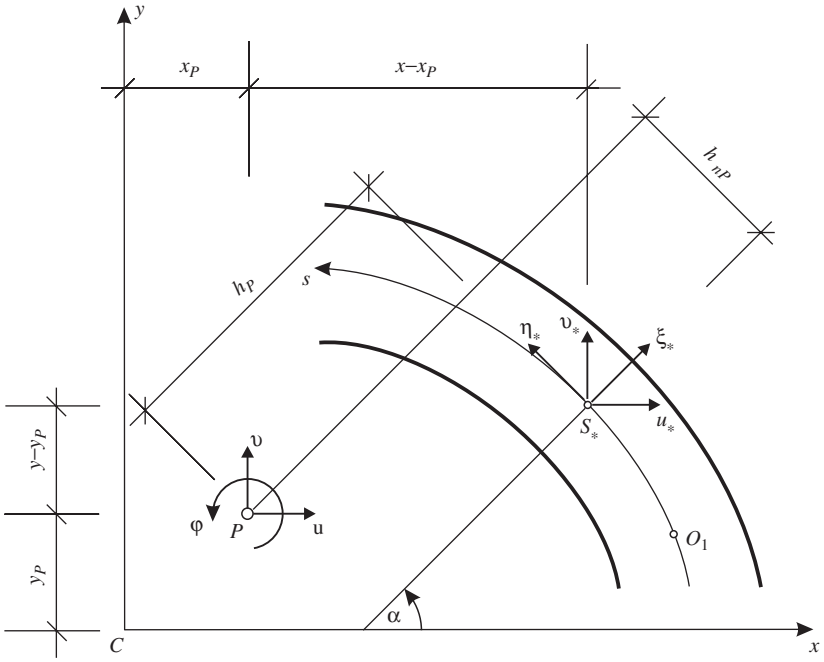

Fig. 1. Section geometry.

coordinates x, y on the contour, where the angle of twist is sufficiently small, are

$$\xi_*(s,z) = v\sin\alpha + u\cos\alpha + \varphi h_{nP},$$
$$\eta_*(s,z) = v\cos\alpha - u\sin\alpha + \varphi h_P, \tag{1}$$

where α denotes the angle between the x and n axes, h_{nP} represents the perpendicular distance from normal at point S_* to the point P given by

$$h_{nP} = (x - x_P)\sin\alpha - (y - y_P)\cos\alpha \tag{2}$$

and h_p represents the perpendicular distance from tangent at point S_* to the point P given by

$$h_P = (x - x_P)\cos\alpha + (y - y_P)\sin\alpha, \tag{3}$$

h_{nP} and h_p are positive when normal **n** and tangent **t**, respectively, are rotating counter clockwise about the pole P, when observed from positive z direction.

The longitudinal displacement w_* of an arbitrary point on contour may be found by using the hypothesis concerning the absence of shearing strain in the middle surface due to bending moment

$$w_* = w - u'x - v'y - \vartheta\omega. \tag{4}$$

The first three terms on the right-hand side of Eq. (4) describe longitudinal displacements of the cross-section as a plane surface. The last term describes the warping of the cross-section, and is given as the product of two functions. The first function $\vartheta(z)$defines the warping intensity and can not be directly expressed as a function of the other parameters used to describe the plane deformation of the cross-section. This function represents a new unknown. The second function $\omega(s)$, being the same for all cross-sections of a member, describes warping of the cross-section qualitatively. This function depends only of geometrical properties of cross-section and is defined with the solution of Saint-Venant's torque

$$\omega(s) = \int_o^s (h_P - \tilde{\tau})\,\mathrm{d}s, \tag{5}$$

where $\tilde{\tau}$ represents Saint Venant shear flow for $G\varphi' = 1$.

Component deformations, different from zero, are given by

$$\varepsilon_z = \frac{\partial w_*}{\partial z} = w' - u''x - v''y - \vartheta'\omega,$$
$$\gamma_{zs} = \gamma_T = \frac{\partial \eta_*}{\partial z} + \frac{\partial w_*}{\partial s} = \varphi' h_P - \vartheta(h_P - \tilde{\tau}). \tag{6}$$

2.3. Stresses and stress resultants

From Hooke's law for normal stress σ_z we get

$$\sigma_z = E\varepsilon_z = E(w' - u''x - v''y - \vartheta'\omega). \tag{7}$$

The shear stresses τ_{zs}, uniformly distributed over the thickness, may be expressed as a sum of the shear stresses τ_T produced by torsion and the shear stresses τ_V produced by bending

$$\tau_{zs} = \tau_T + \tau_V. \tag{8}$$

The shear stresses τ_T can be derived directly from corresponding strains

$$\tau_T = G\gamma_T = G[\varphi' h_P - (h_P - \tilde{\tau})]. \tag{9}$$

The shear stresses τ_V cannot be obtained by simply applying Hooke's law, but only from the axial equilibrium condition.

Reducing the normal stresses on the center of gravity and shear stresses on the pole P we get for stress resultants the following expressions:

$$\begin{aligned}
&\text{Normal force} && N = \iint_F \sigma_z \, \mathrm{d}F,\\
&\text{Bending moment with respect to the } x \text{ axes} && M_x = \iint_F \sigma_z y \, \mathrm{d}F,\\
&\text{Bending moment with respect to the } y \text{ axes} && M_y = -\iint_F \sigma_z x \, \mathrm{d}F,\\
&\text{Shear force in the } x \text{ direction} && V_x = -\iint_F \tau_{zs} \sin\alpha \, \mathrm{d}F,\\
&\text{Shear force in the } y \text{ direction} && V_y = \iint_F \tau_{zs} \cos\alpha \, \mathrm{d}F,\\
&\text{Torsion moment} && T_P = \iint_F \tau_{zs} h_P \, \mathrm{d}F \text{ or } T_P = \iint_F \tau_T h_P \, \mathrm{d}F.
\end{aligned} \tag{10}$$

As it is well known, in the theory of thin-walled beams, we introduce a new generalized force

$$M_\omega = \iint_F \sigma_z \omega \, \mathrm{d}F. \tag{11}$$

This force, due to warping, is called bimoment.

2.4. Equations of motion

The equations of motion of thin-walled beam can be obtained using the principle of virtual displacements. A small element between cross-sections $z_1 = z$ and $z_2 = z+\mathrm{d}z$, Fig. 2, subjected to external loads $\bar{\mathbf{p}}(\bar{p}_x, \bar{p}_y, \bar{p}_z)$ per unit area of midplane is considered.

At any point on the cross-section z_1 acts as a stress vector

$$\boldsymbol{\sigma} = \tau_{zs}\mathbf{t} + \sigma_z \mathbf{i}_z = -\tau_{zs} \sin\alpha \mathbf{i}_x + \tau_{zs} \cos\alpha \mathbf{i}_y + \sigma_z \mathbf{i}_z. \tag{12}$$

The vector of virtual displacements $\delta\mathbf{u}$, which satisfies the necessary continuity conditions and displacement boundary conditions, may be adopted in the same form as a vector of real displacements

$$\begin{aligned}
\delta\mathbf{u} &= \delta u_* \mathbf{i}_x + \delta v_* \mathbf{i}_y + \delta w_* \mathbf{i}_z\\
&= [\delta u - \delta\varphi(y - y_P)]\mathbf{i}_x + [\delta v + \delta\varphi(x - x_P)]\mathbf{i}_y\\
&\quad + (\delta w - \delta u' x - \delta v' y - \delta\vartheta\omega)\mathbf{i}_z.
\end{aligned} \tag{13}$$

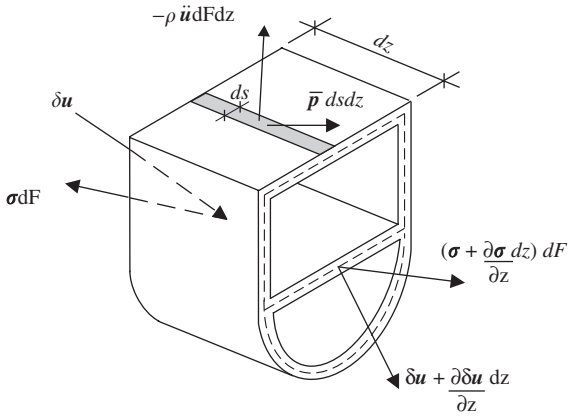

Fig. 2. Differential element of beam.

Virtual displacement parameters are arbitrary functions of coordinates and do not depend upon external loads.

The virtual work expression is

$$\delta\bar{W} + \delta\bar{U} = 0, \tag{14}$$

where $\delta\bar{W}$ = virtual work of external load and inertia forces through virtual displacements $\delta\mathbf{u}$ and $\delta\bar{U}$ = virtual work of actual stresses $\boldsymbol{\sigma}$ realized through virtual strains $\delta\varepsilon = [\delta\varepsilon_z \delta\gamma_T]$.

The virtual work of the external load and inertia forces per unit length of the element is

$$\delta\bar{W} = \iint_F (\boldsymbol{\sigma}'\delta\mathbf{u} + \boldsymbol{\sigma}\delta\mathbf{u}')\,\mathrm{d}F + \int_s \bar{\mathbf{p}}\delta\mathbf{u}\,\mathrm{d}s - \rho\iint_F \ddot{\mathbf{u}}\delta\mathbf{u}\,\mathrm{d}F, \tag{15}$$

where ρ is the density (mass per unit volume), and $\ddot{\mathbf{u}}$ is the acceleration vector given by

$$\begin{aligned}\ddot{\mathbf{u}} &= \ddot{u}_*\mathbf{i}_x + \ddot{v}_*\mathbf{i}_y + \ddot{w}_*\mathbf{i}_z \\ &= [\ddot{u} - \ddot{\varphi}(y - y_P)]\mathbf{i}_x + [\ddot{v} + \ddot{\varphi}(x - x_P)]\mathbf{i}_y \\ &\quad + (\ddot{w} - \ddot{u}'x - \ddot{v}'y - \ddot{\vartheta}\omega)\mathbf{i}_z.\end{aligned} \tag{16}$$

A dot denotes differentiation with respect to time.

Substituting (12), (13) and (16) into (15), the following expression for δW is obtained:

$$\begin{aligned}\delta\bar{W} = \iint_F \Big\{ &-\tau'_{zs}\sin\alpha[\delta u - \delta\varphi(y - y_p)] \\ &+ \tau'_{zs}\cos\alpha[\delta v - \delta\varphi(x - x_p)] \\ &+ \sigma'_z(\delta w - \delta v'y - \delta u'x - \delta\vartheta\omega) \\ &- \tau_{zs}\sin\alpha[\delta u' - \delta\varphi'(y - y_P)] \\ &+ \tau_{zs}\cos\alpha[\delta v' + \delta\varphi'(x - x_P)] \\ &+ \sigma_z(\delta w' - \delta v''y - \delta u''x - \delta\vartheta'\omega)\Big\}\,\mathrm{d}F \\ &+ \int_s \big\{\bar{p}_x[\delta u - \delta\varphi(y - y_P)] \\ &+ \bar{p}_y[\delta v + \delta\varphi(x - x_P)] \\ &+ \bar{p}_z(\delta w - \delta u'x - \delta v'y - \delta\vartheta\omega)\big\}\,\mathrm{d}s \\ &- \rho\iint_F (\delta u_*\ddot{u}_* + \delta v_*\ddot{v}_* + \delta w_*\ddot{w}_*)\,\mathrm{d}F.\end{aligned} \tag{17}$$

The virtual work of the internal load due to the corresponding variation of deformation, per unit length of the element, is

$$\delta\bar{U} = -\iint_F (\sigma_z\delta\varepsilon_z + \tau_T\delta\gamma_T)\,\mathrm{d}F. \tag{18}$$

Using expressions (6) for virtual strains, where real displacement should be replaced by virtual displacement, one gets for δU

$$\delta\bar{U} = -\iint_F \big[\sigma_z(\delta w' - \delta u''x - \delta v''y - \delta\vartheta'\omega) + \tau_T[\delta\varphi' h_P - \delta\vartheta(h_P - \tilde{\tau})]\big]\,\mathrm{d}F. \tag{19}$$

By suitable rearrangement of (17) and (19) in accordance with virtual displacement parameters, the principle of virtual work may be expressed as

$$
\begin{aligned}
&\delta w\left\{\iint_F \sigma_z' \,\mathrm{d}F - \rho \iint_F \ddot{w}_* \,\mathrm{d}F + \int_s \bar{p}_z \,\mathrm{d}s\right\}\\
&+\delta u\left\{-\iint_F \tau_{zs}' \sin\alpha \,\mathrm{d}F - \rho \iint_F \ddot{u}_* \,\mathrm{d}F + \int_s \bar{p}_x \,\mathrm{d}s\right\}\\
&+\delta v\left\{\iint_F \tau_{zs}' \cos\alpha \,\mathrm{d}F - \rho \iint_F \ddot{v}_* \,\mathrm{d}F + \int_s \bar{p}_y \,\mathrm{d}s\right\}\\
&+\delta\varphi\left\{\iint_F \tau_{zs}' h_P \,\mathrm{d}F + \rho \iint_F \left[(y-y_P)\ddot{u}_* - (x-x_p)\ddot{v}_*\right]\mathrm{d}F\right.\\
&\left.+\int_s \left[\bar{p}_y(x-x_P) - \bar{p}_x\left(y-y_P\right)\right]\mathrm{d}s\right\}\\
&-\delta u'\left\{\iint_F (\sigma_z' x + \tau_{zs}\sin\alpha)\,\mathrm{d}F - \rho\iint_F x\ddot{w}_* \,\mathrm{d}F + \int_s \bar{p}_z x \,\mathrm{d}s\right\}\\
&-\delta v'\left\{\iint_F (\sigma_z' y - \tau_{zs}\cos\alpha)\,\mathrm{d}F - \rho\iint_F y\ddot{w}_* \,\mathrm{d}F + \int_s \bar{p}_z y \,\mathrm{d}s\right\}\\
&-\delta\vartheta\left\{\iint_F \left(\sigma_z'\omega - \tau_T(h_P - \tilde{\tau})\right)\mathrm{d}F - \rho\iint_F \omega\ddot{w}_* \,\mathrm{d}F + \int_s \bar{p}_z\omega \,\mathrm{d}s\right\}\\
&-\delta\varphi'\left\{\iint_F (\tau_{zs} - \tau_T)h_P \,\mathrm{d}F\right\} = 0.
\end{aligned}
\tag{20}
$$

To satisfy these equations identically for any virtual displacement parameter $\delta w, \delta u, \delta v, \ldots$ it is necessary that the expressions in the braces vanish. Now, using the expressions for stress resultants (10) and (11), one obtains

$$
\begin{aligned}
&N' - \rho\iint_F \ddot{w}_* \,\mathrm{d}F + p_z = 0,\\
&V_x' - \rho\iint_F \ddot{u}_* \mathrm{d}F + p_x = 0,\\
&V_y' - \rho\iint_F \ddot{v}_* \,\mathrm{d}F + p_y = 0,\\
&T_P' + \rho\iint_F \left[(y-y_P)\ddot{u}_* - (x-x_p)\ddot{v}_*\right]\mathrm{d}F + m_P = 0,\\
&M_y' + V_x + \rho\iint_F x\ddot{w}_* \,\mathrm{d}F + m_y = 0,
\end{aligned}
$$

$$M'_x - V_y - \rho \iint_F y\ddot{w}_* \, dF + m_x = 0,$$

$$M'_\omega - T_P + T_s - \rho \iint_F \omega\ddot{w}_* \, dF + m_\omega = 0, \tag{21}$$

where T_S is Saint Venant torque

$$T_S = \iint_F \tau_T \tilde{\tau} \, dF. \tag{22}$$

The forces V_x and V_y can be eliminated from Eq. $(21)_{5,6}$ in order to obtain five equations

$$N' - \rho \iint_F \ddot{w}_* \, dF + p_z = 0,$$

$$M''_y + \rho \iint_F x\ddot{w}'_* \, dF + \rho \iint_F \ddot{u}_* \, dF - p_x + m'_y = 0,$$

$$M''_x - \rho \iint_F y\ddot{w}'_* \, dF - \rho \iint_F \ddot{v}_* \, dF + p_y + m'_x = 0,$$

$$T'_P + \rho \iint_F \left[(y - y_P)\ddot{u}_* - (x - x_p)\ddot{v}_*\right] dF + m_P = 0,$$

$$M'_\omega - T_P + T_s - \rho \iint_F \omega\ddot{w}_* \, dF + m_\omega = 0. \tag{23}$$

Substituting the expressions for stresses (7) and (9) in Eqs. (10), (11) and (22), the stress resultants can be expressed directly in terms of the displacements

$$\begin{aligned} N &= EFw', \\ M_y &= EI_{xx}u'', \\ M_x &= -EI_{yy}v'', \\ M_\omega &= -EI_{\omega\omega}\vartheta', \\ T_P &= GI_{hh}\varphi' - G(I_{hh} - K)\vartheta, \\ T_S &= GK\varphi', \end{aligned} \tag{24}$$

where K is Saint Venant's torsion constant for thin-walled beam with multicellular cross-section

$$K = \iint_F \tilde{\tau}^2 \, dF = \iint_F \tilde{\tau} h_P \, dF. \tag{25}$$

Now, by substituting (24) into (23) one obtains

$$EFw'' - \rho \iint_F \ddot{w}_* \, dF = -p_z,$$

$$EI_{xx}u'''' + \rho \iint_F x\ddot{w}'_* \, dF + \rho \iint_F \ddot{u}_* \, dF = p_x - m'_y,$$

$$EI_{yy}v'''' + \rho \iint_F y\ddot{w}'_* \, dF + \rho \iint_F \ddot{v}_* \, dF = p_y + m'_x,$$

$$GI_{hh}\varphi'' - G(I_{hh} - K)\vartheta' + \rho \iint_F [(y - y_P)\ddot{u}_* - (x - x_p)\ddot{v}_*]\,\mathrm{d}F = -m_P,$$

$$EI_{\omega\omega}\vartheta'' + G(I_{hh} - K)(\varphi' - \vartheta) + \rho \iint_F \omega\ddot{w}_*\,\mathrm{d}F = m_\omega. \tag{26}$$

Last two equations may be reduced to one by eliminating the unknown ϑ. From Eq. $(26)_4$ follows

$$\vartheta' = \frac{I_{hh}}{I_{hh} - K}\varphi'' + \frac{\rho}{G(I_{hh} - K)} \iint_F [(y - y_P)\ddot{u}_* - (x - x_P)\ddot{v}_*]\,\mathrm{d}F + \frac{m_P}{G(I_{hh} - K)}. \tag{27}$$

Differentiating Eq. $(26)_5$ once with respect to z gives

$$EI_{\omega\omega}\vartheta''' + G(I_{hh} - K)(\varphi'' - \vartheta') + \rho \iint_F \omega\ddot{w}'_*\,\mathrm{d}F = m'_\omega. \tag{28}$$

Eqs. (26-4) and (28) are now added to obtain

$$EI_{\omega\omega}\vartheta''' - GK\varphi'' + \rho \iint_F \omega\ddot{w}'_*\,\mathrm{d}F - \rho \iint_F [(y - y_P)\ddot{u}_* - (x - x_p)\ddot{v}_*]\,\mathrm{d}F = m'_\omega + m_P. \tag{29}$$

Finally, differentiating Eq. (27) twice and substituting in Eq. (29), the following equation is derived:

$$EI^0_{\omega\omega}\varphi'''' - GK\varphi'' + \rho \iint_F \omega\ddot{w}'_*\,\mathrm{d}F - \rho \iint_F [(y - y_P)\ddot{u}_* - (x - x_p)\ddot{v}_*]\,\mathrm{d}F$$
$$+ \rho\frac{EI^0_{\omega\omega}}{GI_{hh}} \iint_F [(y - y_P)\ddot{u}''_* - (x - x_p)\ddot{v}''_*]\,\mathrm{d}F = m'_\omega + m_P - \frac{EI^0_{\omega\omega}}{GI_{hh}}m''_P, \tag{30}$$

where

$$I^0_{\omega\omega} = I_{\omega\omega}\frac{I_{hh}}{I_{hh} - K}. \tag{31}$$

Taking account of Eqs. (16) and (27) one gets the equations

$$EFw'' - \rho F\ddot{w} = -p_z,$$
$$EI_{xx}u'''' - \rho I_{xx}\ddot{u}'' + \rho F\ddot{u} + \rho y_P F\ddot{\varphi} = p_x - m'_y,$$
$$EI_{yy}v'''' - \rho I_{yy}\ddot{v}'' + \rho F\ddot{v} - \rho x_P F\ddot{\varphi} = p_y + m'_x,$$
$$EI^0_{\omega\omega}\varphi'''' - GK\varphi'' - \rho I^0_{\omega\omega}\left(1 + \frac{EI_P}{GI_{hh}}\right)\ddot{\varphi}'' + \frac{\rho^2 I^0_{\omega\omega}}{GI_{hh}}I_P\ddot{\varphi} + \rho I_P\ddot{\varphi}$$
$$+ \frac{\rho^2 I^0_{\omega\omega}}{GI_{hh}}y_P\ddot{u} - \frac{\rho^2 I^0_{\omega\omega}}{GI_{hh}}x_P\ddot{v} + \rho y_P F\ddot{u} - \rho x_P F\ddot{v} - \frac{\rho EI^0_{\omega\omega}}{GI_{hh}}y_P F\ddot{u}'' + \frac{\rho EI^0_{\omega\omega}}{GI_{hh}}x_P F\ddot{v}''$$
$$= m'_\omega + m_P - \frac{EI^0_{\omega\omega}}{GI_{hh}}m''_P. \tag{32}$$

The first equation in Eq. (32), describing axial vibration, is uncoupled from the rest of the system and may be analyzed independently.

The free harmonic transverse and torsional vibrations are defined by the coupled homogeneous Eqs. $(32)_{2,3,4}$. Their solutions are assumed in the following form:

$$\begin{bmatrix} u(z,t) \\ v(z,t) \\ \varphi(z,t) \end{bmatrix} = \begin{bmatrix} U(z) \\ V(z) \\ \Phi(z) \end{bmatrix} \sin pt, \tag{33}$$

where p is the radian frequency and U, V and Φ are amplitudes of the transverse displacements and torsional rotation. Substituting (33) into homogeneous Eq. (32) yields

$$\begin{aligned}
&EI_{xx}U'''' + \rho p^2 I_{xx}U'' - \rho p^2 FU - \rho p^2 y_P F\Phi = 0,\\
&EI_{yy}V'''' + \rho p^2 I_{yy}V'' - \rho p^2 FV + \rho p^2 x_P F\Phi = 0,\\
&EI^0_{\omega\omega}\Phi'''' + \left[\rho p^2 I^0_{\omega\omega}\left(1+\frac{EI_P}{GI_{hh}}\right) - GK\right]\Phi'' - \left(\rho p^2 I_P - \rho^2 p^4 \frac{I^0_{\omega\omega}I_P}{GI_{hh}}\right)\Phi\\
&\quad - \left(\rho p^2 y_P F - \rho^2 p^4 \frac{I^0_{\omega\omega}}{GI_{hh}} y_P F\right)U + \left(\rho p^2 x_P F - \rho^2 p^4 \frac{I^0_{\omega\omega}}{GI_{hh}} x_P F\right)V\\
&\quad + \rho p^2 \frac{EI^0_{\omega\omega}}{GI_{hh}} y_P F U'' - \rho p^2 \frac{EI^0_{\omega\omega}}{GI_{hh}} x_P F V'' = 0.
\end{aligned} \tag{34}$$

In the case of a beam with simply supported ends (fork supports at each end which prevent rotation and can warp freely) the end conditions are

$$\begin{bmatrix} U \\ V \\ \Phi \end{bmatrix} = \begin{bmatrix} 0 \\ 0 \\ 0 \end{bmatrix}, \qquad \begin{bmatrix} U'' \\ V'' \\ \Phi'' \end{bmatrix} = \begin{bmatrix} 0 \\ 0 \\ 0 \end{bmatrix}. \tag{35}$$

These requirements are satisfied by taking

$$\begin{bmatrix} U(z) \\ V(z) \\ \Phi(z) \end{bmatrix} = \begin{bmatrix} C_U \\ C_V \\ C_\Phi \end{bmatrix} \sin \lambda_n z, \tag{36}$$

where C_U, C_V and C_Φ are constants and $\lambda_n = n\pi/L$, $n = 1, 2$, etc.

Substituting (36) into (34) results in

$$\begin{aligned}
&\left[EI_{xx}\lambda_n^4 - \rho p^2\left(\lambda_n^2 I_{xx} + F\right)\right]C_U - \rho p^2 y_P F C_\Phi = 0,\\
&\left[EI_{yy}\lambda_n^4 - \rho p^2\left(\lambda_n^2 I_{yy} + F\right)\right]C_V + \rho p^2 x_P F C_\Phi = 0,\\
&\left[EI^0_{\omega\omega}\lambda_n^4 + GK\lambda_n^2 - \rho p^2\left(\lambda_n^2 I^0_{\omega\omega} + \frac{\lambda_n^2 I^0_{\omega\omega} EI_P}{GI_{hh}} + I_P\right) + \rho^2 p^4 \frac{I^0_{\omega\omega}I_P}{GI_{hh}}\right]C_\Phi\\
&\quad + \left[-\rho p^2 y_P F\left(1 + \frac{\lambda_n^2 EI^0_{\omega\omega}}{GI_{hh}}\right) + \rho^2 p^4 \frac{I^0_{\omega\omega} y_P F}{GI_{hh}}\right]C_U + \left[\rho p^2 x_P F\left(1 + \frac{\lambda_n^2 EI^0_{\omega\omega}}{GI_{hh}}\right) - \rho^2 p^4 \frac{I^0_{\omega\omega} x_P F}{GI_{hh}}\right]C_V = 0.
\end{aligned} \tag{37}$$

In order to find non-trivial solutions for C_U, C_V and C_Φ the detrminant of the above system must be equal zero, i.e.

$$\begin{bmatrix} \lambda_n^4 I_{xx} - (\lambda_n^2 I_{xx} + F)p_* & 0 & -y_P F p_* \\ 0 & \lambda_n^4 I_{yy} - (\lambda_n^2 I_{yy} + F)p_* & x_P F p_* \\ \chi y_P F p_*^2 - y_P F(1+\chi\lambda_n^2)p_* & -\chi x_P F p_*^2 + x_P F(1+\chi\lambda_n^2)p_* & \chi I_P p_*^2 - (\lambda_n^2 I^0_{\omega\omega} + \chi\lambda_n^2 I_P + I_P)p_* + \lambda_n^4 I^0_{\omega\omega} + \lambda_n^2(GK/E) \end{bmatrix} = 0 \tag{38}$$

where

$$\chi = \frac{EI^0_{\omega\omega}}{GI_{hh}}, \qquad p_* = \frac{\rho}{E}p^2. \tag{39}$$

Then we obtain the following algebraic frequency equation of the fourth order

$$ap_*^4 + bp_*^3 + cp_*^2 + dp + e = 0 \tag{40}$$

with the coefficients

$$\begin{aligned}
a &= (\lambda_n^2 I_{xx} + F)(\lambda_n^2 I_{yy} + F)\chi I_P - (\lambda_n^2 I_{xx} + F)\chi x_P^2 F^2 - (\lambda_n^2 I_{yy} + F)\chi y_P^2 F^2,\\
b &= (x_P^2 I_{xx} + y_P^2 I_{yy})\lambda_n^4 \chi F^2 - [(\lambda_n^2 I_{yy} + F)I_{xx} + (\lambda_n^2 I_{xx} + F)I_{yy}]\lambda_n^4 \chi I_P\\
&\quad + [(\lambda_n^2 I_{xx} + F)x_P^2 F^2 + (\lambda_n^2 I_{yy} + F)y_P^2 F^2](1 + \chi\lambda_n^2) - (\lambda_n^2 I_{xx} + F)(\lambda_n^2 I_{yy} + F)(\lambda_n^2 I_{\omega\omega}^0 + \lambda_n^2 \chi I_P + I_P),\\
c &= (\lambda_n^2 I_{xx} + F)(\lambda_n^2 I_{yy} + F)\left(\lambda_n^4 I_{\omega\omega}^0 + \lambda_n^2 \frac{GK}{E}\right) - (1 + \chi\lambda_n^2)(\lambda_n^4 x_P^2 F^2 I_{xx} + \lambda_n^4 y_P^2 F^2 I_{yy})\\
&\quad + \lambda_n^8 I_{xx} I_{yy} \chi I_P + [\lambda_n^4 I_{xx}(\lambda_n^2 I_{yy} + F) + \lambda_n^4 I_{yy}(\lambda_n^2 I_{xx} + F)](\lambda_n^2 I_{\omega\omega}^0 + \lambda_n^2 \chi I_P + I_P),\\
d &= -\lambda_n^8 I_{xx} I_{yy}(\lambda_n^2 I_{\omega\omega}^0 + \lambda_n^2 \chi I_P + I_P) - \left(\lambda_n^4 I_{\omega\omega}^0 + \lambda_n^2 \frac{GK}{E}\right)[\lambda_n^4 I_{xx}(\lambda_n^2 I_{yy} + F) + \lambda_n^4 I_{yy}(\lambda_n^2 I_{xx} + F)],\\
e &= \lambda_n^{12} I_{xx} I_{yy} I_{\omega\omega}^0 + \lambda_n^{10} \frac{GK}{E} I_{xx} I_{yy}.
\end{aligned} \tag{41}$$

Note that frequency equation of Vlasov model, Prokić [17], may be obtained by introducing into Eq. (38): $I_{\omega\omega}^0 = I_{\omega\omega}$ and $\chi = 0$.

3. Numerical examples

Three numerical examples are given here to illustrate the accuracy of the method derived in this paper.

The geometrical properties of the cross-sections of the beam, in the examples below, were calculated using the computer program given in Ref. [18].

3.1. Example 1

To verify the results obtained by the analytical solution based on Benscoter's theory a simply supported box-girder bridge with span length of 45.72 m is considered, Fig. 3. It allows a comparison with results given by Huang et al. [3], using finite element method, and Hamed and Frostig [19].

The geometrical and material properties of the beam are

$$\begin{aligned}
E &= 2.779 \times 10^7\,\mathrm{kNm^{-2}},\\
G &= 1.068 \times 10^7\,\mathrm{kNm^{-2}},\\
F &= 7.20\,\mathrm{m^2},\\
I_{xx} &= 52.0320\,\mathrm{m^4},\\
I_{yy} &= 12.1860\,\mathrm{m^4},\\
I_{\omega\omega} &= 9.7985\,\mathrm{m^6},\\
K &= 23.8356\,\mathrm{m^4},\\
I_{hh} &= 32.6149\,\mathrm{m^4},\\
I_P &= 64.8185\,\mathrm{m^4},\\
\rho &= 2.54\,\mathrm{kN\,s^2\,m^{-4}},\\
x_P &= 0.0,\\
y_P &= -0.2888\,\mathrm{m}.
\end{aligned}$$

The first five natural frequencies obtained from the present theory are shown in Table 1 together with those given in Refs. [3,19].

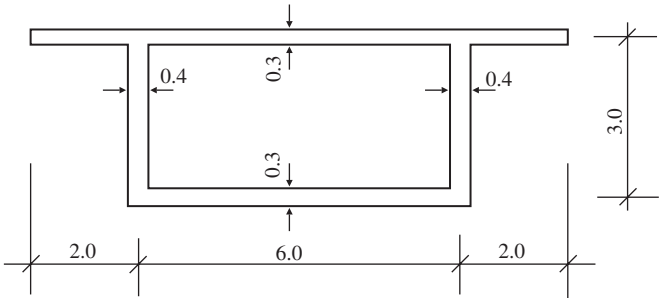

Fig. 3. Cross-section layout for Example 1.

Table 1
Natural frequencies (Hz) of beam studied as Example 1

Mode no.	Mode shape	Present solutions	Reference [5]	Reference [16]
1	Vertical flexure	3.202	3.220	3.172
2	Horizontal flexure	6.524	6.644	6.294
3	Second vertical flexure	12.659	12.962	12.067
4	Torsion	13.628	14.961	11.860
5	Second torsion	27.840	19.975	15.184

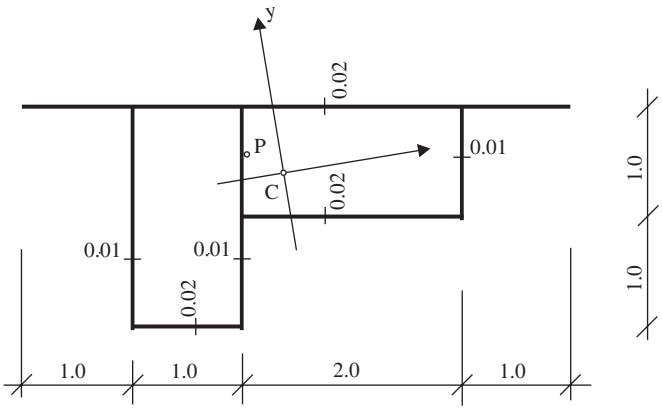

Fig. 4. Cross-section layout for Example 2.

The analytical results of Benscoter's theory and the models proposed in Refs. [3,19] agree well in the lower natural frequencies. As we move towards higher vibration modes, differences in natural frequencies increase, especially in the torsional modes, due to distortion effects of the bridge cross-section.

3.2. Example 2

A simply supported beam with a general cross-section shown in Fig. 4 is investigated.

The geometrical and mechanical properties of the beam are as follows:

$$E = 2.1 \times 10^8\,\mathrm{kNm^{-2}},$$
$$G = 8.07 \times 10^7\,\mathrm{kNm^{-2}},$$
$$F = 0.21\,\mathrm{m^2},$$
$$I_{xx} = 0.329097\,\mathrm{m^4},$$
$$I_{yy} = 0.0960282\,\mathrm{m^4},$$
$$I_{\omega\omega} = 0.0133434\,\mathrm{m^6},$$
$$K = 0.0926546\,\mathrm{m^4},$$
$$I_{hh} = 0.140630\,\mathrm{m^4},$$
$$I_P = 0.45844\,\mathrm{m^4},$$
$$\rho = 78.5/9.81 = 8.002\,\mathrm{kN\,s^2\,m^{-4}},$$
$$x_P = -0.33536\,\mathrm{m},$$
$$y_P = 0.21491\,\mathrm{m}.$$

For $n = 1$, 2 and 3 four natural frequencies of a simply supported thin-walled beam, were determined. Four numerical values characterize four different internal modes of natural frequencies: predominantly flexural mode, in x and y directions, predominantly torsional mode and predominantly warping mode. In Table 2, the results are compared with results of Vlasov's theory presented by Prokić [17], for different slenderness ratios of thin walled beam.

3.3. Example 3

As a third example, the simply supported beam with cross-section shown in Fig. 5 is considered.

The geometrical and mechanical properties of the beam are given in Table 3. In Table 4, the analytical solutions of Benscoter's model are compared with analytical solutions of Vlasov's model.

In this example the influence of distortional behavior of cross-sections on vibration characteristic of box girder is also analyzed, changing the wall thickness ($t = 2$, 4 and 6 cm) and span length ($L = 10$ and 15 m). Numerical solutions by the present study, based on the assumption of undeformed cross-section, are compared with FEM solutions analyzed by 600 shell elements of Tower 5 [20]. The model is provided with

Table 2
Natural frequencies (Hz) of beam studied as Example 2

External mode	$L = 5$ m			$L = 10$ m			$L = 50$ m		
	Benscoter theory	Vlasov theory	Error (%)	Benscoter theory	Vlasov theory	Error (%)	Benscoter theory	Vlasov theory	Error (%)
$n = 1$	146.40	148.04	1.13	51.89	51.90	0.01	2.17	2.17	0.00
	209.68	209.89	0.10	75.05	75.11	0.08	14.01	14.01	0.00
	319.66	319.67	0.00	96.23	96.23	0.00	14.86	14.86	0.00
	1090.79	—	—	993.35	—	—	959.80	—	—
$n = 2$	319.30	350.12	9.65	146.40	148.04	1.13	8.65	8.65	0.00
	676.30	676.69	0.06	209.68	209.89	0.10	15.85	15.85	0.00
	867.94	867.96	0.00	319.66	319.67	0.00	29.92	29.93	0.00
	1410.71	—	—	1090.79	—	—	964.06	—	—
$n = 3$	498.54	620.40	24.44	231.59	241.66	4.35	19.31	19.31	0.00
	1223.25	1223.75	0.04	424.02	424.31	0.07	34.73	34.73	0.00
	1417.81	1417.82	0.00	589.54	589.55	0.00	45.71	45.72	0.01
	1819.50	—	—	1234.83	—	—	971.13	—	—

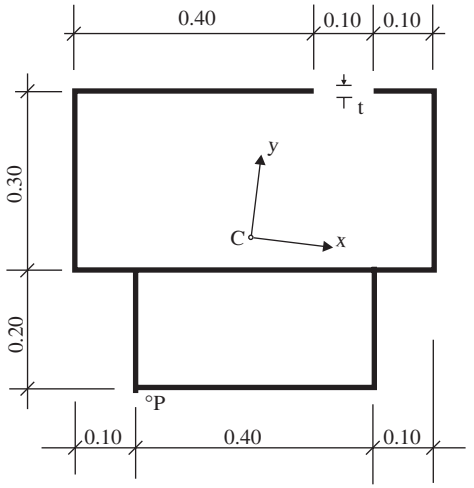

Fig. 5. Cross-section layout for Example 3.

Table 3
Geometric and material properties of beam studied in Example 3

t (cm)	2.0	4.0	6.0
E (kN m^{-2})	2.10×10^{8}	2.10×10^{8}	2.10×10^{8}
G (kN m^{-2})	8.07×10^{7}	8.07×10^{7}	8.07×10^{7}
ρ (kN s^{-2} m^{-4})	8.002	8.002	8.002
F (m^2)	0.05	0.10	0.15
x_P (m)	−0.13278	−0.13246	−0.13192
y_P (m)	−0.29245	−0.29220	−0.29178
I_{xx} (m^4)	0.00218815	0.00438033	0.00658057
I_{yy} (m^4)	0.00156318	0.00313234	0.00471343
$I_{\omega\omega}$ (m^6)	0.00018136	0.00036343	0.00054690
K (m^4)	0.00043333	0.00090666	0.00146000
I_{hh} (m^4)	0.00538981	0.01077750	0.01616120
I_P (m^4)	0.00890920	0.01780532	0.02667477

Table 4
Natural frequencies (Hz) of beam studied as Example 3 ($t = 2$ cm), comparison with Vlasov theory

External mode	$L = 5$ m			$L = 10$ m			$L = 15$ m		
	Benscoter theory	Vlasov theory	Error (%)	Benscoter theory	Vlasov theory	Error (%)	Benscoter theory	Vlasov theory	Error (%)
$n = 1$	52.88	53.12	0.44	14.06	14.06	0.00	6.29	6.29	0.00
	59.72	59.83	0.18	16.01	16.01	0.00	7.30	7.30	0.00
	150.52	152.14	1.08	59.86	59.88	0.04	37.75	37.75	0.00
	2714.72	—	—	2660.77	—	—	2650.50	—	—
$n = 2$	176.66	180.76	2.32	52.88	52.95	0.13	24.68	24.68	0.00
	229.00	229.26	0.12	59.72	59.75	0.04	27.67	27.68	0.01
	456.23	461.52	1.16	150.52	150.96	0.29	85.59	85.67	0.09
	2909.93	—	—	2714.72	—	—	2675.00	—	—
$n = 3$	350.43	374.67	6.92	107.95	108.87	0.85	52.88	52.95	0.13
	498.21	499.08	0.17	130.91	131.04	0.10	59.72	59.75	0.05
	886.09	901.46	1.73	283.93	286.00	0.73	150.52	150.96	0.29
	3187.15	—	—	2799.60	—	—	2714.72	—	—

Table 5
Natural frequencies (Hz) of beam studied as Example 3, comparison with FE $L = 10\,\text{m}$, $t = 2\,\text{cm}$

Dominant mode shape	Present solution	Finite element Number of transverse diaphragms (n)			
		$n = 0$	$n = 2$	$n = 4$	$n = 6$
Vertical	14.06	12.88	13.60	13.99	14.01
Horizontal	16.01	13.56	15.80	15.93	15.95
Torsion	59.86	32.74	40.15	55.03	55.79
Second vertical	52.88	31.16	38.30	47.52	50.08
Second horizontal	59.72	40.20	51.89	55.18	57.22

Table 6
Natural frequencies (Hz) of beam studied as Example 3, comparison with FE $L = 10\,\text{m}$, $t = 4\,\text{cm}$

Dominant mode shape	Present solution	Finite element Number of transverse diaphragms (n)			
		$n = 0$	$n = 2$	$n = 4$	$n = 6$
Vertical	14.08	13.68	13.99	14.07	14.09
Horizontal	16.05	15.10	15.99	16.02	16.04
Torsion	60.91	44.60	56.34	57.28	57.50
Second vertical	53.13	45.54	47.44	50.13	51.13
Second horizontal	59.85	48.68	57.18	57.63	57.97

Table 7
Natural frequencies (Hz) of beam studied as Example 3, comparison with FE $L = 10\,\text{m}$, $t = 6\,\text{cm}$

Dominant mode shape	Present solution	Finite element Number of transverse diaphragms (n)			
		$n = 0$	$n = 2$	$n = 4$	$n = 6$
Vertical	14.12	13.92	14.09	14.12	14.12
Horizontal	16.11	15.57	16.08	16.10	16.11
Torsion	62.63	51.57	59.49	59.57	59.73
Second vertical	53.53	48.48	50.20	51.20	51.71
Second horizontal	60.07	52.70	58.10	58.22	58.36

Table 8
Natural frequencies (Hz) of beam studied as Example 3, comparison with FE $L = 15\,\text{m}$, $t = 2\,\text{cm}$

Dominant mode shape	Present solution	Finite element Number of transverse diaphragms (n)			
		$n = 0$	$n = 2$	$n = 4$	$n = 6$
Vertical	6.29	6.18	6.30	6.30	6.30
Horizontal	7.30	6.99	7.31	7.31	7.31
Torsion	37.75	24.67	32.58	34.93	35.27
Second vertical	24.68	21.36	22.10	23.56	24.06
Second horizontal	27.67	23.27	26.86	27.02	27.14

Table 9
Natural frequencies (Hz) of beam studied as Example 3, comparison with FE $L = 15\,\text{m}$, $t = 4\,\text{cm}$

Dominant mode shape	Present solution	Finite element Number of transverse diaphragms (n)			
		$n = 0$	$n = 2$	$n = 4$	$n = 6$
Vertical	6.30	6.30	6.31	6.31	6.31
Horizontal	7.31	7.24	7.31	7.32	7.32
Torsion	38.50	31.51	36.36	36.53	36.61
Second vertical	24.74	23.44	23.93	24.19	24.37
Second horizontal	27.75	25.88	27.37	27.40	27.46

Table 10
Natural frequencies (Hz) of beam studied as Example 3, comparison with FE $L = 15\,\text{m}$, $t = 6\,\text{cm}$

Dominant mode shape	Present solution	Finite element Number of transverse diaphragms (n)			
		$n = 0$	$n = 2$	$n = 4$	$n = 6$
Vertical	6.31	6.31	6.35	6.36	6.36
Horizontal	7.34	7.31	7.37	7.38	7.38
Torsion	39.72	34.79	38.20	38.23	38.23
Second vertical	24.82	24.08	24.37	24.46	24.54
Second horizontal	27.87	26.72	27.59	27.61	27.63

some intermediate transverse diaphragms ($n = 0$, 2, 4 and 6) allowing the variability of the distortion rigidity studied. The diaphragms have regular distances along the longitudinal axis of the beam and are supposed to be of infinite rigidity in-plane and zero out-plane.

The first five natural frequencies of free vibration obtained by Benscoter's theory and FEM are compared in Tables 5–10. The corresponding first five normal shapes (predominant vertical, horizontal, second vertical, second horizontal and torsion), for $L = 15\,\text{m}$, $t = 2\,\text{cm}$ and $n = 2$, are shown in Figs. 6(a)–(e). The results given illustrate that:

a. As we move towards higher vibration modes, differences in natural frequencies increase, especially in the torsional modes.
b. Results of Benscoter's theory are in good agreement with real vibration behavior of thin-walled beam with increasing distortional rigidity of cross-sections and slenderness of the beam.
c. Larger discrepancies between Benscoter results and FEM results of real structures that consist of deformable closed sections may rise as a consequent of the Benscoter's assumption that the cross-section is perfectly rigid in its own plane. That happens in the case of less distortion rigidity of cross-section or when the beams are constructed without sufficient number of diaphragms that cause the section shape to distort.

4. Conclusion

In the case of simply supported beams of non-deformable closed cross-sections, the exact solution for natural frequencies of free harmonic vibrations was derived. Even in the case of thin-walled beam with deformable cross-sections, when the effects of distortion on the dynamic behavior of thin-walled beam are considerable, the solution based on Benscoter's theory may be useful from the viewpoint of initial beam design and can be used to validate the other approximate methods.

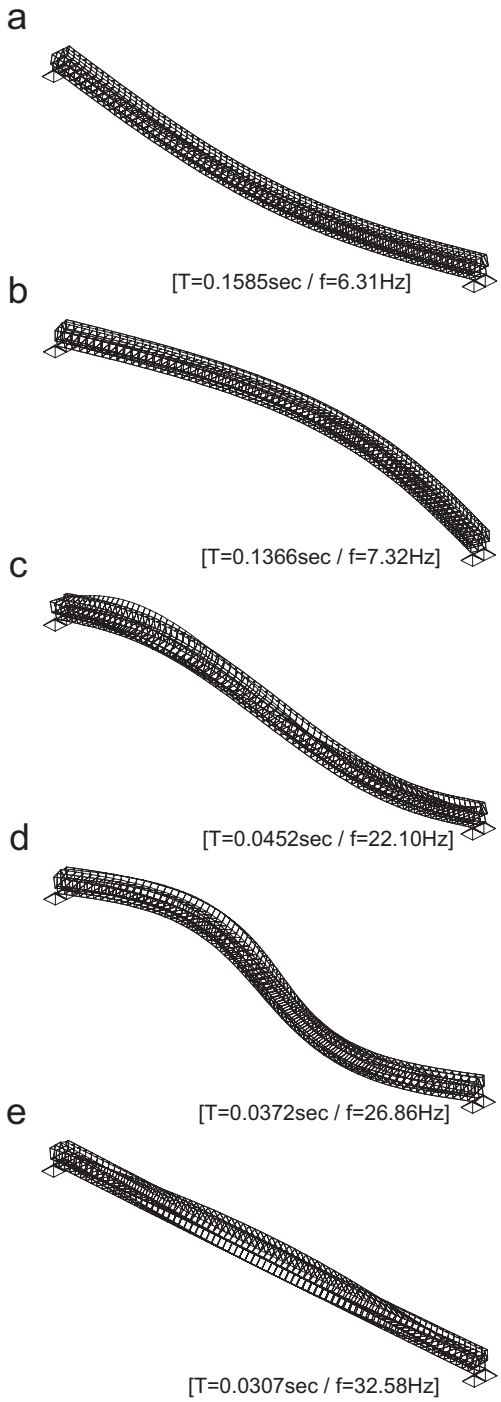

Fig. 6. First five normal mode shapes of Example 3. ($L = 15\,\text{m}$, $t = 2\,\text{cm}$, $n = 2$): (a) mode 1-vertical; (b) mode 2-horizontal; (c) mode 3-s vertical; (d) mode 4-s horizontal; (e) mode 5-torsion.

Examination of Tables 2 and 4 shows that we have not much differences in the fundamental frequency for Benscoter's and Vlasov's model. As we move toward higher vibration modes and toward less slender beams differences in natural frequencies for two models increase.

It may be supposed that it is reasonable enough to extend this conclusions to the beams with other boundary conditions, but this demands further examination.

Acknowledgments

The present work has been supported by Ministry of Science and Environmental Protection of the Republic of Serbia (Project 144037).

Appendix A

The values that determine geometrical properties of cross-section are given by

$$I_{xx} = \iint_F x^2 \,\mathrm{d}F,$$

$$I_{yy} = \iint_F y^2 \,\mathrm{d}F,$$

$$I_{\omega\omega} = \iint_F \omega_P^2 \,\mathrm{d}F,$$

$$I_{hh} = \iint_F h_P^2 \,\mathrm{d}F,$$

$$I_P = \iint_F \left[(x - x_P)^2 + (y - y_P)^2\right] \mathrm{d}F.$$

Externally applied loads and moments per unit length of a beam are as follows:

$$p_x = \int_s \bar{p}_x \,\mathrm{d}s, \quad p_y = \int_s \bar{p}_y \,\mathrm{d}s, \quad p_z = \int_s \bar{p}_z,$$

$$m_x = \int_s \bar{p}_z y \,\mathrm{d}s, \quad m_y = -\int_s \bar{p}_z x \,\mathrm{d}s, \quad m_P = \int_s [\bar{p}_y(x - x_P) - \bar{p}_x(y - y_P)] \,\mathrm{d}s,$$

$$m_\omega = \int_s \bar{p}_z \omega_P \,\mathrm{d}s.$$

References

[1] M.J. Mikkola, J. Paavola, Finite element analysis of box girder, *Journal of the Structural Division, ASCE* 106 (1980) 1343–1357.
[2] A.G. Razaqpur, H.G. Li, Thin-walled multicell box girder finite element, *Journal of Structural Engineering, ASCE* 117 (10) (1991) 2953–2971.
[3] D. Huang, T. Wang, M. Shahawy, Vibration of thin-walled box-girder bridges excited by vehicles, *Journal of Structural Engineering, ASCE* 121 (9) (1995) 1330–1336.
[4] J.H. Kim, Y.Y. Kim, One-dimensional analysis of thin-walled closed beams having general cross-section, *International Journal for Numerical Methods in Engineering* 49 (2000) 653–668.
[5] Y.Y. Kim, J.H. Kim, Thin-walled closed box beam element for static and dynamic analysis, *International Journal for Numerical Methods in Engineering* 45 (1999) 473–490.
[6] Y.K. Cheung, M.S. Cheung, *Free Vibration of Curve and Straight Beam Slab or Box Girder Bridges*, Vol. 32 (2), IABS Publications, 1972, pp. 41–55.
[7] S.G. Hutton, Y.K. Cheung, Dynamic response of single span highway bridges, *Earthquake Engineering and Structural Dynamics* 7 (1979) 543–553.
[8] D. Hartman, M. Neummann, Structural optimization of a box girder bridge by means of the finite strip method, in: C.A. Brebbia, S. Hernandez (Eds.), *Computer Aided Optimum Design of Structures*, Computational Mechanics Publications, Southampton, UK, 1989, pp. 337–346.

[9] N. Taysi, M. Ozakca, Free vibration analysis and shape optimization of box-girder bridges in straight and curved planform, *Engineering Structures* 24 (2002) 625–637.
[10] M.S. Cheung, A. Megnounit, Parametric study of design variations on the vibration modes of boxgirder bridges, *Canadian Journal of Civil Engineering* 18 (5) (1991) 789–798.
[11] K.M. Sennah, J.B. Kennedy, Dynamic characteristics of simply supported curved composite multi-cell bridges, *Canadian Journal of Civil Engineering* 24 (4) (1997) 621–636.
[12] L.T. Stavridis, G.T. Michaltsos, Eigenfrequency analysis of thin-walled girders curved in plan, *Journal of Sound and Vibration* 227 (2) (1999) 383–396.
[13] V. Kristek, *Theory of Box Girders*, Wiley, New York, 1979.
[14] P.O. Friberg, Coupled vibrations of beams—an exact dynamic element stiffness matrix, *International Journal for Numerical Methods in Engineering* 19 (1983) 479–493.
[15] J.R. Banerjee, Development of an exact dynamic stiffness matrix for free vibration analysis of a twisted Timoshenko beam, *Journal of Sound and Vibration* 270 (1–2) (2004) 379–401.
[16] K. Moon-Young, K. Nam II, Y. Hee-Taek, Exact dynamic and static stiffness matrices of shear deformable thin-walled beam-columns, *Journal of Sound and Vibration* 267 (1) (2003) 29–55.
[17] A. Prokić, On triply coupled vibrations of thin-walled beams with arbitrary cross-section, *Journal of Sound and Vibration* 279 (2005) 723–737.
[18] A. Prokić, Computer program for determination of geometrical properties of thin-walled beams with open-closed section, *Computers & Structures* 74 (2000) 705–715.
[19] E. Hamed, Y. Frostig, Free vibrations of multi-girder and multi-cell boxbridges with transverse deformations effects, *Journal of Sound and Vibration* 279 (2005) 699–722.
[20] *Tower 5, Professional Integrated Software—Finite Element Analysis and Design of Structures*, Radimpex, Beograd.